A novel hybrid carbon materials-modified electrochemical sensor used for detection of gallic acid

Achour TERBOUCHE[a,*], Soumeya BOULAHIA[a,b] Sarah MECERLI[a,b], Chafia AIT-RAMDANE-TERBOUCHE[a], Hakim BELKHALFA[a], Djamila GUERNICHE[a,c], Moussa SEHAILIA[a], Khaldoun BACHARI[a], Djillali MEZAOUI[d], Didier HAUCHARD[e]

[a]*Centre de Recherche Scientifique et Technique en Analyses Physico-chimiques (CRAPC), BP384, Bou-Ismail, RP 42004, Tipasa, Algeria.*

[b]*Faculté de Chimie, Université USTHB, 16111 Algers, Algeria*

[c]*Laboratoire d'Electrochimie-corrosion, Métallurgie et Chimie Minérale, Faculté de Chimie, Université USTHB, 16111 Algers, Algeria*

[d]*Laboratoire Sciences des Matériaux, Faculté de Chimie, Université USTHB, 16111 Algers, Algeria*

[e]*Univ Rennes, ENSC Rennes, CNRS, ISCR – UMR6226, F-35000 Rennes, France.*

[*]*Corresponding author: achour_t@yahoo.fr ; achour.terbouche@crapc.dz ; Tel.: +213.660 37 01 15, fax: +213.24.325.774*

Abstract

Novel hybrid carbon materials such as activated carbon-carbon nanotubes (AC-CNTs) and carbon spheres/activated carbon-carbon nanotubes (CSs/AC-CNTs) based on activated carbon (AC) derived from the pits of Algerian date palm have been prepared and characterized. In addition, the carbon paste electrodes based on graphite carbon (GC) and cavity microelectrode (CME) modified with these hybrid materials were used to detect gallic acid at pH=7 using square wave voltammetry method (SWV). The conductivity measurements revealed that CSs/AC-CNTs is more conducting than AC-CNTs. SWV measurements showed that the oxidation current was directly proportional to the concentrations of gallic acid (from 0 to 0.00536 M) with the lowest limit of detection (LOD), reaching 6.43 µM and 3.64 µM using GC/CSs/AC-CNTs electrode and CME/GC/CSs/AC-CNTs sensor, respectively. The

reproducibility and the stability of the studied sensor were confirmed by the relative standard deviation of the oxidation current response of gallic acid ($RSD_{Reproducibility}$ =1.44% and $RSD_{Stability}$=3.7%).

Keywords: Hybrid carbon materials; Electrical conductivity measurement; Cavity microelectrode sensor; Gallic acid analysis.

1. Introduction

Over the last few decades, much attention has been devoted to the application of nano-structured materials, in particular carbon nanotubes. The application of CNTs and carbon derivatives has been widely carried out in several fields of chemical analysis [1-4]. A combination of the interactions between CNTs and the metal-ligand system was found to be the most important recognition mechanism [5-7]. This class of compounds is commonly known to facilitate the transfer of electrons between the electroactive species and the working electrodes, but their major disadvantage is the prohibitive cost of these metal catalyst systems. For this, it would be wise to look for efficient and low cost products such as hybrid activated carbons.

Activated carbons are multifunctional materials that have interesting properties such as electrochemistry, catalysis, sorption, ion exchange and complexation. For these advantages, these materials are widely used in various applications [8]. In recent years, considerable efforts have been invested in improving the electrochemical properties of activated carbons by introducing carbonaceous materials such as carbon nanotubes, graphene, and carbon black [9, 10]; this not only increases the conductivity and shortens the electron transfer distances, but also increases the active surface area and improves the utilization rate of the active material.

Generally, chemically modified electrodes are formed by binding the mono- or multilayer molecules on the surface of the electrode [11, 12]. The change in the nature of the surface of

the material was found to improve the selectivity and sensitivity of the electrode [13]. Different electrodes modified with insoluble electroactive compounds have been used in analytical chemistry [14-17], electrochemical and kinetic methods. They are widely useful in all of these are highly useful for the detection and monitoring of electroactive species [18-20]. Composites of multiwalled carbon nanotube and porous activated carbon were fabricated to determine different analytes simultaneously using electrochemical techniques [21, 22]. Also, single and double thread activated carbon fibers were used for pH sensing [23]. In addition, the composites of carbon spheres were used to prepare non-enzymatic glucose sensors [24], as well as in the development of electrochemical sensing platform based on nitrogen-doped hollow carbon spheres for sensitive and selective isoprenaline detection [25].

To the best of our knowledge, the utilization of modified electrodes derived from activated carbon, sourced from date pits in the detection of gallic acid, as antioxidant compound, has not been covered by the scientific literature before. The latter is considered as potential antioxidant and its proper intake may be good for health, it is used as an additive in foods, drugs and cosmetics. In addition, gallic acid is a type of polyphenol contained in natural plants, fruits and vegetables, and has antiallergic, antimutagenic and antistamenic activities [26, 27].

In this work, novel hybrid carbon materials and modified electrodes designed from different carbon compounds based on activated carbon obtained from the pits of Algerian date palm have been developed to detect the presence of gallic acid in solution. The purpose of this work is divided into two folds; initially, the synthesis, characterization, electrical conductivity measurements and electrochemical properties of novel hybrid carbon materials based on activated carbon from the pits of date palm (AC), CSs and CNTs were studied. Secondly, the carbon paste electrodes and CME modified with these new hybrid materials have been developed in order to determine the amount of gallic acid in an aqueous solution.

2. Materials and methods

2. 1. Apparatus and reagent

Fourier Transform Infrared Spectroscopy (FT-IR) and Attenuated Total Reflectance (ATR) spectra were recorded using a BRUKER ALPHA-T/P spectrometer (Ettlingen, Germany) in the spectral range of 4000-400 cm^{-1}. Scanning Electron Microscopy with Energy Dispersive X-Ray Analysis (SEM-EDX) characterization of the synthesized carbon products was carried out using scanning electron microscope FEI QUANTA 250 (Salem, OR, USA). The apparatus used to carry out X-Ray Diffractograms (XRD) and Thermogravimetric Analysis (TGA) are Bruker D8 Advance A25 diffractometer (Ettlingen, Germany) and SDT Q600 TA Instrument (Delaware, USA), respectively. All conductivity measurements were recorded using a GW Instek model GDM-8255 multimeter (Taipei, Taiwan). Electrochemical measurements were performed using Potentiostat/Galvanostat Metrohm Autolab 302N (Utrecht, The Netherlands) and a cell containing a reference electrode (Ag/AgCl) and a counter electrode (vitreous carbon). All measurements were recorded using "Nova 1.9" software.

All reagents and solvents used to prepare the measurement solutions were of high purity and analytical grade purchased from Sigma–Aldrich (USA) (Multi-Walled Carbon Nanotubes: MWCNTs and gallic acid), Merck (Germany) or Fluka (Switzerland) Chemical Companies (HNO_3, H_2O_2, NaH_2PO_4/Na_2HPO_4).

2. 2. Preparation of carbon compounds

2. 2. 1. Activated carbon

Our activated carbon is obtained from 141.36 g of pits of Algerian date palm (188 pits of Deglet Nour). Carbonization of the pits was performed after washing them several times with distilled water and further optimization of the carbonization temperature (carbonization time of each tested temperature: 1 hour). The resulting black product (mass: 43.109 g; yield:

65.9%; calc. temp. 450 °C) was cooled to room temperature, washed with distilled water and dried under vacuum in an oven for 48 hours at 50 °C. The resulting coal was activated using potassium hydroxide (1M), the product was then filtered, washed with distilled water and dried in an oven at 60 °C.

2. 2. 2. Activation of CNTs

CNTs (MWCNTs): 5-10 nm diameter, length: 5-30 µm and high purity (99%)) were purchased from sigma-Aldrich and were activated using the following procedure:

1 g of carbon nanotubes was mixed with 100 mL of concentrated nitric acid (1 M), the mixture was stirred mechanically for 24 hours. The resulting product was filtered, washed with distilled water and dried at 60 °C. Finally, 0.8 g of activated CNTs have been recovered after the activation step using HNO_3.

The activated CNTs were not soluble in water or other organic solvents such as DMSO and DMF.

2. 2. 3. Preparation of CSs

Carbon spheres were synthesized following chemical vapor deposition (CVD) method, using acetylene as a carbon source [28, 29]. The synthesis procedure of CSs is as follows [30]:

A quartz tubular reactor was placed horizontally in an oven at 900 °C, acetylene was passed through to effect pyrolysis (flow: 100 mL/min) in the presence of nitrogen (N_2 flow: 40 mL/min) for 2 hours to generate the desired carbon spheres. The yield of the reaction was 15%.

2. 2. 4. Preparation of AC-CNTs material

To prepare AC-CNTs, 1.4 g of AC was mixed with 0.7 g of activated carbon nanotubes in distilled water, the resulting mixture was stirred for 2 hours. Finally, the resulting product was filtered, dried at 60 °C and placed in an oven at 500 °C for 2 hours.

2. 2. 5. Preparation of CSs/AC-CNTs compound

CSs/AC-CNTs was synthesized by the following procedure:

A solution of carbon spheres was prepared by dissolving a mass of 0.15 g of CSs in 60 mL of DMSO. A mass of 1.5 g of AC-CNTs was added to this solution (carbon spheres) and the resulting mixture was stirred for further 24 hours. Finally, the obtained product was filtered, washed and dried at 60 °C.

2. 2. 6. Preparation of modified electrodes

The modified carbon paste electrodes based on graphite carbon (GC) were prepared as follows:

300 mg of graphite powder and 50 mg of each synthesized product (AC, AC-CNTs and CSs/ AC-CNTs) were mixed and grounded in a mortar for 15 min. Five drops of paraffin oil (Nujol) were added to the obtained homogeneous mixture. The prepared carbon paste was embedded in a 2 mm diameter quartz glass tube, and the same amount of graphite powder was introduced into the upper part of the tube to improve the conductivity of the electrode. The electrical contact was made using a copper wire.

To prepare the new sensor based on the modified cavity microelectrode (CME/GC/CSs/AC-CNTs), the CME (Scheme 1) was filled with active material by pressing the electrode tip into the GC/CSs/AC-CNTs powder previously prepared.

Before each measurement, the CME was washed by ultrasonic method using successively HNO_3 solution (1 M), H_2O_2 (30%) and deionised water.

2. 2. 7. Electrochemistry

The electrochemical behavior of the modified CME and carbon paste electrodes was assessed by CV and SWV experiments in a buffer solution (NaH_2PO_4/Na_2HPO_4: 0.1M; pH=7) with KNO_3 (0.1 M) as support electrolyte. The SWV study was carried out within the potential range between -0.5 V and 0.73 V, frequency = 1 Hz and potential increment = 5 mV. In order to check the stability of the electrode materials, successive scans were recorded at 20 mV/s before each measurement.

To study the electrochemical behavior of all carbonaceous compounds, such as electrochemical response as a function of scan rate as well as the charge transfer, we used a more suitable electrode surface (carbon paste electrode) to assess the best electrochemical response among the three compounds (AC, AC-CNTs and CSs/AC-CNTs). After these studies, the best compound will be tested for the detection of gallic acid using CME.

3. Results and discussion

3. 1. Characterization of the compounds

3. 1. 1. Infrared spectra

Infrared spectroscopy was used to identify the different functional groups present in carbon compounds.

The most important vibration bands of the various carbon compounds are shown in Fig. S1 and Table 1.

Comparative study of FTIR spectra of all carbon products showed the disappearance, appearance and shift of vibrational bands corresponding to certain functional groups. The

intense peaks observed in the range of 3400-3450 cm^{-1} are attributed to the stretching vibration of OH bonds in hydroxyl and carboxylic acid groups [31, 32]. The peaks recorded between 2820 and 2980 cm^{-1} are assigned to asymmetric and symmetric CH in CH_2 and CH_3 groups of aliphatic, olefin and aromatic groups [31-34]. The bands appearing between 1752 and 1733 cm^{-1} are assigned to carbonyl group (υC=O) vibrations in hydroxyl, carboxylic acids and anhydride groups. Analysis of FTIR spectra showed low-intensity bands in the range of 1510-1595 cm^{-1}, attributed to C=C stretching vibrations in the aromatic rings [31, 32]. The peaks observed between 1424 to 1460 cm^{-1} are due to the deformation vibration of O-H and C-H in hydroxyl, phenol and olefin groups, while the peak located around 1380 cm^{-1} corresponds to methyl groups [31, 32].

The peaks observed in the range of 1000-1250 cm^{-1} are assigned to the vibration of C-O bonds that can be appeared after activation of compounds [35, 36].

Comparative studies between the FTIR spectrum of AC and that of AC-CNTs showed that the vibration peaks of O-H and C=O were shifted to high energies, while the vibration band of C=C was shifted towards the low energies, explaining the modification of the environment of the functional groups of each carbon compound due to the formation of hydrogen bonds.

Compared with that observed on the spectrum of AC-CNTs, the recorded CSs/AC-CNTs spectrum showed that the vibration bands of O-H and C=C were shifted towards high and low energies, respectively. In addition, the stretching vibration of the carbonyl group (υC=O) has disappeared in the spectrum of CSs/AC-CNTs. These results (shift and disappear of bands) indicate the modification of the environment of the functional groups and the formation of covalent bonds between CSs and AC-CNTs, confirming the formation of hybrid carbon compound (CSs/AC-CNTs).

It should be noted that these results were also confirmed using attenuated reflectance spectroscopy (ATR) (not shown here).

3. 1. 2. SEM- EDX characterization

Results showing the SEM characterization of the various carbon products are presented in Fig. 1. It has been noted that all carbon compounds presented a remarkable variation in surface morphology. SEM photographs of the surface of activated carbon revealed the formation of small-sized pores and channels. Fig. 1a, b showed homogeneity on the surface of treated coal (AC). With regards to the SEM photographs recording for CSs/AC-CNTs (Fig. 1c, d), clusters of carbon nanotubes which are in the form of very dense fibers were observed on the activated carbon surface. These photographs showed insertion of the carbon spheres into the pores of the activated carbon, thus confirming the adsorption of CSs on AC-CNTs.

EDX analysis of the coal (not shown here) demonstrated the presence is composed mainly of carbon (53.77%), nitrogen (28.27%), oxygen (16.91%) and trace elements as impurity (1.05%), while that of the activated carbon contained mainly 73% of carbon and large amount of oxygen resulting from the activation of the coal. The EDX analysis reported in Fig. S2a showed that AC-CNTs compound contained 79% of carbon and 16% of oxygen. The addition of carbon spheres to AC-CNTs increased the oxygen content (22.03%) and decreased that of the carbon content (68.61%) (Fig. S2b).

3. 1. 3. X-ray diffraction (XRD)

XRD makes it possible to identify the nature of the crystalline and amorphous phases present in a solid. However, several crystalline meshes must follow each other to form visible diffraction lines. If the number of meshes constituting the crystallites is small, the diffraction lines will appear wide. This property makes it possible in certain cases to determine the size of the crystallites.

The angle (2θ) range used in this study is between 10° and 80°. The results of X-ray diffraction peaks of the obtained carbon based products are shown in Fig. 2.

Recordings showed an amorphous structure for all the carbon based products with a low crystallinity observed in the range 10 to 45°.

For the untreated coal, the diffractograms showed a peak at 23° and another peak at 41°. Diffraction patterns of the different activated products (AC, AC-CNTs, CSs/AC-CNTs) were almost of the same shape with diffraction peaks between 24-25° and 41-43°, which are respectively attributed to the presence of graphite carbon and dehydrated hemicellulose. After activation of the raw coal, the main peak moved from 23° to 24°, which demonstrated that the activation process has been well performed.

By adding CNTs to activated carbon, the peak at 24° became more intense than that of AC and shifted to about 25°. After adsorption of the carbon spheres on the AC-CNTs compound, the peak of AC-CNTs became wider while it was also shifted on the CSs/AC-CNTs diffractogram.

3. 1. 4. Thermal measurement

Thermogravimetric analysis is an analytical technique that consists of measuring the change in the mass of a sample as a function of temperature [37]. The decomposition temperature strongly depends on the type of material used and the employed method for the chemical treatment. In this part of the present work, the thermogravimetric study of carbon materials is performed in the temperature range of 0-1000 °C at a heating rate of 10 °C/min. The thermal analysis results of these products are shown in Fig. 3. The shape of the TGA curves of the different carbonized compounds is identical to that obtained for the other activated carbons already studied.

The evolution in mass loss of activated carbon during heat treatment can be divided into four stages: the first mass loss (0.57%), observed in the temperature range 60 to 110 °C was due to the release of the adsorbed water molecules [38]. The other three losses of masses,

corresponding to the values of 3.31%, 17.1% and 28.39%, observed in the temperature ranges of 110-347 °C, 347-657 °C and 657-936 °C, are due to the decomposition of activated carbon into pectin, hemicellulose, cellulose, lignin and carbon oxides (CO and CO_2) [39, 40]. TGA of AC-CNTs indicated a mass loss of 13.9% in the temperature range 482-974 ^{o}C, which correspond to the weight loss of oxygen containing materials in the temperature range of 482-974 °C [41]. In addition, the thermogram of AC-CNTs showed also a mass loss of 1.5% in the temperature range 74.8-227 °C, which was due to the dehydration of water molecules [42]. The evolution in the mass loss of CSs/AC-CNTs product during heat treatment can be divided into three stages: the first mass loss (6.94%) in the temperature range of 72 to 217 °C is attributed to the release of the adsorbed water molecules [43]. The second loss of mass (17.83%) in the temperature range 217-653 °C is due to the decomposition of residual lignin, cellulose, pectin and hemicellulose [44], while the products are exposed to higher temperatures, the surface groups decompose, producing CO and CO_2 in the temperature range 653-949 °C [45, 46].

3. 1. 5. Electrical conductivity measurement

In this part, the graphite was used as a reference material to study the electrical conductivity of the synthetized hybrid carbon compounds.

The conductivity measurements vs. temperature for all prepared products are shown in Fig. 4. The curves shown in Figs. 4a, 4b demonstrated the evolution of the conductivity (S) of GC, AC, AC-CNTs and CSs/AC-CNTs. Analysis of these results revealed that conductivity increases with temperature and that activated carbon was an insulating product, whereas AC-CNTs compound was found to be more conductive than AC.

The data recorded in Figs. 4a, 4b show that the presence of CSs in the AC-CNTs compound improved its conductivity. The electrical conductivity is classified as follows: GC> CSs/AC-CNTs > AC-CNTs > AC.

Fig. 4c shows log S vs.1000/T in the temperature range of 482-600 °C. By applying the Arrhenius equation below [47, 48], the activation energies of the different compounds can be calculated from the slopes of lines $logS = f(\frac{1000}{T})$.

$$S = S_0 e^{\frac{-\Delta E}{KT}}$$

With *S*: Conductivity (S. m^{-1}) ;

S_0: Resistivity (Ω. m) ;

ΔE: Activation energy of the reaction (eV) ;

K: Boltzmann constant (K = 8.67×10^{-5} eV/K) ;

T: Temperature (K).

The evaluated values of activation energies related with the various carbon products show that CSs/AC-CNTs compound has the lowest activation energy (E_a=0.183 eV) when compared with other products AC-CNTs (E_a=0.195 eV) AC (E_a=0.353 eV), ZnO matrix with CNTs and graphene nanoplate (GNP) mixture (E_a=0.230-0.392 eV) [49], thermally cured carbon black–epoxy (CB–EP) (E_a=0.253-0.707 eV) [50] and sub-superficial graphite-diamond-graphite junction (E_a=0.217 eV) [51].

Knowing that the activation energy represents the minimum amount of energy needed to initiate a chemical reaction, we can conclude that CSs/AC-CNTs compound has better activity, which makes it a decisive element in the subsequent application of sensors based on CSs/AC-CNTs product.

3. 2. Electrochemical study

3. 2. 1. Electrochemical behavior of modified carbon paste *electrodes*

The electrochemical behavior of the modified carbon paste GC/AC electrode was examined and compared with those of GC/AC-CNTs and GC/CSs/AC-CNTs electrodes in order to evaluate the difference between these electrodes in a buffer medium. The voltammograms of all compounds obtained at scan rate of 20 mV/s are shown in Fig. 5.

The voltammograms recorded in Fig. 5a showed that all electrodes had no electrochemical response in the absence of gallic acid. However, in the presence of gallic acid (Fig. 5b), all electrodes presented an electrochemical response in the form of an oxidation wave (E_a) between 0.25 and 0.5 V, assigned to the oxidation of gallic acid. The recorded voltammograms showed that the oxidation of gallic acid was performed easily on the surface of GC/CSs/AC-CNTs electrode giving the highest oxidation current (i_a=461.65 µA; E_{pa}=0.36 V). On the other hand, the oxidation of gallic acid was carried out with difficulty on the surface of GC/AC (i_a=102.31µA; E_{pa}=0.64 V) and GC/AC-CNTs (i_a=220.03 µA; E_{pa}=0.41 V) electrodes. This result showed the effect of the active surface area of CSs on the efficiency of GC/CSs/AC-CNTs electrode.

3. 2. 2. Electrochemical behavior versus scan rate of modified carbon paste *electrodes in the presence of gallic acid*

Fig. 6a showed the voltamperograms obtained using GC/CSs/AC-CNTs electrode at different scan rates in a phosphate buffer solution (pH = 7) containing KNO_3 (0.1 M) in the presence of gallic acid (0.01M). It was clearly observed that increasing the scan rate prompted increases in the current intensity of the anodic peaks. Indeed, increasing the scan rate (v) was accompanied by a shift in potentials towards the most positive values, indicating that the electro-oxidation process of gallic acid was irreversible.

Studying of the variation in current vs. square root of scan rate *(i_p= f ($v^{1/2}$))* (Fig. 6 b, Fig. S3a) and the variation of the potential vs. logv *(E=f (logv))* (Fig. 6 c, Fig. S3b and Fig. S4) can give information on the nature of the limiting step occurring in the electrochemical process as well as providing us with an insight about the reaction mechanism happening at the surface of the electrode.

Fig. 6 b and Fig. S3a showed that the current intensity was directly proportional to the square root of scan rate, suggesting that the processes corresponding to the oxidation peaks are controlled by the diffusion phenomenon of the species in solution.

On the other hand, the potential is found to be proportional to the logarithm of the scanning rate, this value was moved towards the most positive region revealing that the oxidation-reduction processes are slow and irreversible.

3. 2. 3. Calculation of the charge transfer coefficient (α)

By referring to the Tafel line which defines an irreversible electrochemical process [52], the value of the charge transfer coefficient (α) is deduced from the slope of the equation below:

$$E_p = \frac{b}{2} logv + K$$

With $\frac{b}{2}$ is the slope of straight line and K is constant.

$$\frac{b}{2} = \frac{2.303RT}{n(1-\alpha)F}$$

Assuming that the number of electrons involved in the electrochemical system is n = 2 (reaction below), we obtain the values of calculated α reported in Table 2.

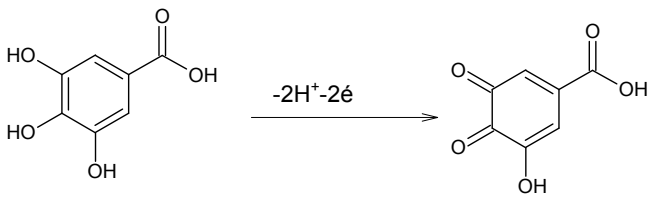

The charge transfer coefficient determined using the carbon paste electrode modified with CSs/AC-CNTs material (GC/CSs/AC-CNTs: α=0.77) indicated a better electro-catalytic mechanism for the oxidation of gallic acid in the presence of a very homogeneous surface (GC/AC-CNTs: α=0.76; GC/AC: α=0.75).

3. 2. 4. Electrochemical behavior of modified electrodes using square wave voltammetry (SWV)

Measurements were carried out by SWV after the introduction of the modified CME and paste carbon electrodes into a solution containing a phosphate buffer (pH = 7) and KNO_3 (0.1 M) in the absence and presence of gallic acid. When compared with the results obtained in the electrochemical study section using cyclic voltammetry, the SWV study (Fig. S5) showed that the anodic waves are sharper and better defined (better resolution) than those obtained by CV. Comparison of the SW voltammograms recorded by each modified electrode (in the absence and the presence of gallic acid 0.01M) (Fig. S5) showed the presence of an oxidation wave between E_a=0.28V and E_a=0.32V in the presence of gallic acid. The oxidation wave of this species, located at E_{pa}= 0.31 V with GC/AC (i_a= 36.29 μA) electrode underwent a small shift towards the lower potentials when compared with GC/AC-CNTs (E_{pa}= 0.32 V; i_a=95.98 μA) and GC/CSs/AC-CNTs (E_{pa}= 0.28 V; i_a=129.06 μA) electrodes. The last result showed that the process of anodic oxidation of gallic acid takes place easily on the surface of the electrode containing CSs/AC-CNTs compound. This finding was confirmed by evaluating the electrochemical behavior of the modified cavity microelectrode with CSs/AC-CNTs in the presence of gallic acid (Fig. 7).

3. 3. Detection of gallic acid

To determine *LOD* of gallic acid using each electrode, calibration plots of current vs. concentration of gallic acid have been plotted and their slopes have been evaluated. The general equation used to determine this limit of detection [53-55] is:

$$LOD = \frac{3s}{m}$$

With s: the standard deviation of the oxidation currents; m: the slope of the calibration plot of the current intensity versus concentration of gallic acid $(i = a \times [GA] + b)$.

In order to evaluate the influence of the concentration of gallic acid on the electrochemical response of the different electrodes, square wave voltammograms have been recorded for different concentrations of gallic acid (Fig. 8 and Fig. 9). In the absence of this species in the measuring solution, all modified electrodes do not show any electrochemical response. However, the addition of gallic acid showed the presence of an oxidation peak in the potential range 0-0.5 V.

Based on the recorded SW voltammograms, a linear relationship was obtained between the oxidation current and the concentration of gallic acid over a wide range of concentrations ranging from 0 to 0.00536 M. The equations of the calibration lines determined using GC/AC, GC/AC-CNTs, GC/CSs/AC-CNTs modified paste electrodes and CME/GC/CSs/AC-CNTs sensor are: $y = 9.1867 \times 10^{-4}x + 6.4608 \times 10^{-9}$ $(R^2 = 0.992)$; $y = 0.00111x + 5.9213 \times 10^{-9}$ $(R^2 = 0.997)$, $y = 0.0014x + 6.5236 \times 10^{-9}$ $(R^2 = 0.995)$ and $y = 8.233 \times 10^{-4}x + 3.201 \times 10^{-7}$ $(R^2 = 0.994)$, respectively.

The values of the calculated limits of detection (Table 2) revealed that the LODs for gallic acid, determined by the different electrodes, are arranged in the following order: CME/GC/CSs/AC-CNTs (3.64 μM) < GC/CSs/AC-CNTs (6.43 μM) < GC/AC-CNTs (8.11

μM) < GC/AC (22.86 μM). These results revealed that CME/GC/CSs/AC-CNTs electrode has better detection of gallic acid than any other electrodes previously published in literature around pH =7 and in concentration range from 0 to 0.00536 M, e.g., GCE/CeO_2 nanoparticles (LOD=11.9 μM) [56], screen-printed carbon electrodes (LOD=23-102 μM) and redox microsensors (LOD=109 μM) [57]. Based on these results, we find that the CME/GC/CSs/AC-CNTs electrode exhibited more considerable electrochemical performance toward gallic acid analysis of in aqueous solution.

In this study, the analytical advantage of the CME/GC/CS/AC-CNTs electrode for analyzing gallic acid in aqueous solution was demonstrated. Then, in order to study the reproducibility of the sensor, four CME/GC/CS/AC-CNTs type electrodes were prepared under the same measurement conditions, and each one was evaluated by detecting 0.00192 M gallic acid. According to Figure 10, the calculations revealed that RSD % of the oxidation peak current of gallic acid was about 1.44 %. However, to check the accuracy and stability of the modified electrode (CME/GC/CSs/AC-CNTs) at pH=7, two measurements were performed to detect 0.00192 M gallic acid, using the same electrode after ten days of storage at room temperature. The relative standard deviation of the actual gallic acid response was about 3.7 %.

4. Conclusion

In this present work, novel hybrid carbon materials (AC-CNTs and CSs/AC-CNTs) based on activated carbon derived from the pits of Algerian date palm were prepared and characterized by electrical conductivity and different spectroscopic and analytical methods. The synthetically modified carbon paste electrodes and the modified cavity microelectrode with these hybrid compounds were used to determine and quantify gallic acid using square wave voltammetry method.

The electrical conductivity measurements vs. temperature showed that CSs/AC-CNTs hybrid carbon material has the lowest activation energy of E_a=0.183 eV and better activity compared to other products (AC-CNTs: E_a=0.195 eV; AC: E_a=0.353 eV). In addition, the charge transfer coefficient evaluated using GC/CSs/AC-CNTs modified paste electrode revealed a better electro-catalytic oxidation mechanism of gallic acid than that calculated using GC/AC-CNTs electrode. The SWV study showed that the cavity microelectrode modified with GC/CSs/AC-CNTs hybrid carbon material exhibited a lower limit of detection of gallic acid (LOD=3.64 µM) than those evaluated using other modified electrodes around the same linear concentration range at pH = 7. The reproducibility of the studied sensor (CME/GC/CSs/AC-CNTs) showed that RSD % of the oxidation peak current of gallic acid was about 1.44 %. Finally, the accuracy and stability studies of this new electrode at pH=7 revealed that the relative standard deviation of gallic acid response was about 3.7 %.

Acknowledgements

The authors would like to thank the ministry of higher education and scientific research (MESRS), Algeria and the general directorate for scientific research and technological development (DGRSDT), Algeria for supporting the present research.

We are very grateful to Dr. Djahida LERARI and Dr. Amel BOUDJEMAA (Divisions: Material sciences and environement at CRAPC) for providing us with CSs and CNTs products.

The French UMEC network of the CNRS is warmly acknowledged for providing the cavity microelectrode.

References

[1] Bagheri, H.; Khoshsafar, H.; Amidi, S.; Hosseinzadeh, A.Y. Fabrication of an electrochemical sensor based on magnetic multi-walled carbon nanotubes for the determination of ciprofloxacin. Anal. Methods. 2016, 8, 3383-3390. DOI: https://doi.org/10.1039/C5AY03410H

[2] Wang, B.; Dou, S.; Li, W.; Gao, Y. Multifunctional reduced graphene oxide/carbon nanotubes/epoxy resin nanocomposites based on on carbon nanohybrid perform. Soft Materials. 2019. DOI : https://doi.org/10.1080/1539445X.2019.1688833

[3] Bagheri, H.; Talemi, R.P.; Afkhami, A. Gold nanoparticles deposited on fluorine-doped tin oxide surface as an effective platform for fabricating a highly sensitive and specific digoxin aptasensor. RSC Adv. 2015, 5, 58491-58498. DOI: https://doi.org/10.1039/C5RA09402J

[4] Kumanek, B.; Stando, G.; Wróbel, P.S.; Krzywiecki, M.; Janas, D. Thermoelectric properties of compositefilms from multi-walled carbon nanotubes and ethyl cellulose doped with heteroatoms. Synth. Met. 2019, 257, 116190. DOI: https: // doi. org/ 10.1016/ j. synthmet.2019.116190

[5] Siswana, M.; Ozoemena, K.I.; Nyokong, T. Electrocatalytic Detection of Amitrole on the Multi-Walled Carbon Nanotube – Iron (II) tetra-aminophthalocyanine Platform. Sensors 2007, 8, 5096–5105. DOI: https://doi.org/10.3390/s8085096

[6] Bianco, A.; Hoebeke, J.; Godefroy, S.; Chaloin, O.; Pantarotto, D.; Briand, J.P.; Muller, S.; Prato, M.; Partidos, C.D. Cationic carbon nanotubes bind to CpG oligodeoxynucleotides and enhance their immunostimulatory properties. J. Am. Chem. Soc. 2005[a], 127, 58–59. DOI: https://doi.org/10.1021/ja044293y

[7] Ajayan, P.M. Nanotubes from Carbon. Chem. Rev. 1999, 99, 1787–1799. DOI: https://doi.org/10.1021/cr970102g

[8] Volperts, A.; Plavniece, A.; Dobele, G.; Zhurinsh, A.; Kruusenberg, I.; Kaare, K.; Locs, J.; Tamasauskaite-Tamasiunaite, L.; Norkus, E. Biomass based activated carbons for fuel cells. Renew. Energy 141 (2019) 40-45. DOI : https://doi.org/10.1016/j.renene.2019.04.002

[9] Jangid, K.; Sahu, R.P.; Pandey,R.; Chen, R.; Zhitomirsky, I.; Puri, I.K. Multiwalled Carbon Nanotubes Coated with Nitrogen–Sulfur Co-Doped Activated Carbon for Detecting Fenitrothion. ACS Appl. Nano Mater. 2021, 4, 4781-4789. DOI: https://doi.org/ 10.1021/acsanm.1c00376

[10] Tigari, G.; Manjunatha, J.G. A surfactant enhanced novel pencil graphite and carbon nanotube composite paste material as an effective electrochemical sensor for determination of riboflavin. J. Sci.: Adv. Mater. Devices 2020, 5, 56-64. DOI : https://doi.org/10.1016/j.jsamd.2019.11.001

[11] Terbouche, A.; Ait-Ramdane-Terbouche, C. ; Djebbar, S. ; Benali-Baitich, O.; Hauchard, D. Effectiveness study of sensor based on modified cavity microelectrode by Algerian humic acid-polyaniline composites using square wave voltammetry. Sens. Actuators B. 2012, 169, 297-304. DOI: https://doi.org/10.1016/j.snb.2012.04.085

[12] Giasmera, M.J.; Sevilia, M.T.; Procopio, J.R. Potentiometric carbon paste senors for lead(II) based on dithiodibenzoic and mecaptobenzoic acids. Anal. Sci. 2006, 22, 405–412. DOI: https://doi.org/10.2116/analsci.22.405

[13] Ait Ramdane-Terbouche, C.; Terbouche, A.; Djebbar, S.; Hauchard, D. Electrochemical sensors using modified electrodes based on copper complexes formed with Algerian humic acid modified with ethylenediamine or triethylenetetramine for determination of nitrite in water. Talanta. 2014, 119, 214–225. DOI: https://doi.org/10.1016/j.talanta.2013.10.049

[14] Ojani, R.; Raoof, J.B., Norouzi, B. Electropolymerization of N-methylaniline in the presence of sodium dodecylsulfate and its application for electrocatalytic reduction of nitrite. J. Mater. Sci. 2009, 44, 4095-4103. DOI: https://doi.org/10.1007/s10853-009-3591-8

[15] Xing, Y.; Wu, G.; Ma, Y. ; Yu, Y.; Yuan, X.; Zhu, X.; Electrochemical detection of bisphenol B based on poly(Prussian blue)/carboxylated multiwalled carbon nanotubes composite modified electrode. Measurement. 2019, 148, 106940. DOI: https: // doi.org/ 10.1016/j.measurement .2019.106940

[16] Mohammadi, S.Z.; Beitollahi, H.; Kaykhaii, M.; Mohammadizadeh, N.; Tajik, S.; Hosseinzadeh, R. Simultaneous determination of droxidopa and carbidopa by carbon paste electrode functionalized with $NiFe_2O_4$ nanoparticle and 2-(4-ferrocenyl-[1, 2, 3] triazol-1-yl)-1-(naphthalen-2-yl) ethanone. Measurement. 2020, 155, 107522. DOI: https: // doi.org/ 10.1016/j.measurement.2020.107522

[17] Bagheri, H.; Afkhami, A.; Khoshsafar, H.; Rezaei, M.; Sabounchei, S.J.; Sarlakifar, M. Simultaneous electrochemical sensing of thallium, lead and mercury using a novel ionic liquid/graphene modified electrode. Anal. Chim. Acta. 2015, 870, 56–66. DOI: https://doi.org/10.1016/j.aca.2015.03.004

[18] Badea, M.; Modugno, F.; Floroian, L.; Tit, D.M.; Restani, P.; Bungau, S.; Iovan, C.; Badea, G.E.; Aleya, L. Electrochemical strategies for gallic acid detection: Potential for application in clinical, food or environmental analyses. Sci. Total Environ. 2019, 672, 129-140. DOI: https://doi.org/10.1016/j.scitotenv.2019.03.404

[19] Hanko, M.; Švorc, L.; Planková, A.; Mikuš, P. Overview and recent advances in electrochemical sensing of glutathione. Anal. Chim. Acta. 2019, 1062, 1-27. DOI: https://doi.org/10.1016/j.aca.2019.02.052

[20] Challier, L.; Miranda-Castro, R.; Marchal, D.; Noël, V.; Mavré, F.; Limoges, B. Kinitic Rotating Droplet Electrochemistry: A Simple and Versatile Method for Reaction Progress

Kinitic Analysis in Microliter. J. Am. Chem. Soc. 2013, 135, 14215-14228. DOI: https://doi.org/10.1021/ja405415q

[21] Oularbi, L.; Turmine, M.; El Rhazi, M. Preparation of novel nanocomposite consisting of bismuth particles, polypyrrole and multi-walled carbon nanotubes for simultaneous voltammetric determination of cadmium(II) and lead(II). Synth. Met. 2019, 253, 1-8. DOI: https://doi.org/10.1016/j.synthmet.2019.04.011

[22] Zhang, T.; Jin, H.; Fang, Y.; Guan, J.B.; Ma, S.J. ; Pan, Y. ; Zhang, M.; Zhu, H.; Liu, X.D.; Du, M.L. Detection of trace Cd^{2+}, Pb^{2+} and Cu^{2+} ions via porous activated carbon supported palladium nanoparticles modified electrodes using SWASV. Mat. Chem. Phys. 2019, 225, 433-442. DOI: https://doi.org/10.1016/j.matchemphys.2019.01.010

[23] Ahmed, N.M.; Sabah, F.A.; Kabaa, E.A.; Myint, M.T.Z. Single- and double-thread activated carbon fibers for pH sensing. Mat. Chem. Phys. 2019, 221, 288-294. DOI: https://doi.org/10.1016/j.matchemphys.2018.09.059

[24] Chen, J.; Yin, H.; Zhou, J.; Gong, J.; Wang, L.; Zheng, Y.; Nie, Q. Non-enzymatic glucose sensor based on nickel nitride decorated nitrogen doped carbon spheres (Ni3N/NCS) via facile one pot nitridation process. J. Alloys Comp. 2019, 797, 922-930. DOI: https://doi.org/10.1016/j.jallcom.2019.05.234

[25] Shahrokhian, S.; Panahi, S.; Salimian, R. An electrochemical sensing platform based on nitrogen-doped hollow carbon spheres for sensitive and selective isoprenaline detection. J. Electroanal. Chem. 2019, 847, 113196. DOI: https://doi.org/10.1016/j.jelechem.2019.113196

[26] Fukumoto, L.R.; Mazza, G. Assessing antioxidant and prooxidant activities of phenolic compounds. J. Agr. Foodchem. 2000, 48, 3597-3604. DOI: https://doi.org/10.1021/jf000220w

[27] Kroes, B.H.; Van Den Berg, A.J.; Quarles Van Ufford, H.C.; Van Dijk, H.; Labadie, R.P. Anti-inflammatory activity of gallic acid. Plant. Med. 1992, 58, 499-504. DOI: https://doi.org/10.1055/s-2006-961535

[28] Serp, P.H.; Feurer, R.; Kalck, P.H.; Kihn, Y.; Faria, J.L.; Figueiredo, J.L. A chemical vapour deposition process for the production of carbon nanospheres. Carbon. 2001, 39, 621–626. DOI: https://doi.org/10.1016/S0008-6223(00)00324-9

[29] Xiong, H.; Moyo, M.; Motchelaho, M.A.M.; Jewell, L.L.; Coville, N.J. Fischer–Tropschsynthesis over model iron catalysts supported on carbons pheres: the effect of iron precursor, support pretreatment, catalys tpreparation method and promoters. Appl. Catal. A: Gen. 2010, 388, 168–178. DOI: https://doi.org/10.1016/j.apcata.2010.08.039

[30] Boudjemaa, A.; Mokrani, T.; Bachari, K.; Covill, N.J. Electrochemical and photo-electrochemical properties of carbon spheres prepared via chemical vapor deposition. Mater. Sci. Semicond. Process. 2015, 30, 456–461. DOI : http://dx.doi.org/10.1016/j.mssp.2014.10.050

[31] Durán-Valle, C.J.; Gómez-Corzo, M. ; Pastor-Villegas, J.; Gómez-Serrano, V. Study of cherry stones as raw material in preparation of carbonaceous adsorbents. J. Anal. Appl. Pyrolysis. 2005, 73, 59–67. DOI: https://doi.org/10.1016/j.jaap.2004.10.004

[32] Artur, P.T. The influence of activated carbon surface chemical composition on the adsorption of acetaminophen (paracetamol) in vitro: Part II. TG, FTIR, and XPS analysis of carbons and the temperature dependence of adsorption kinetics at the neutral pH. J. Colloid surfaces A: Physicochem. Eng. Aspects. 2001, 177, 23-45. DOI: https: // doi.org/ 10.1016/S0927-7757(00)00594-X

[33] Lua, A.C.; Guo, J. Preparation and characterization of activated carbons from oil-palm stones for gas-phase adsorption. J. Colloid surfaces A: Physicochem. Eng. Aspects. 2001, 179, 151-162. DOI: https://doi.org/10.1016/S0927-7757(00)00651-8

[34] Moreno-Castilla, C.; Carrasco-Marín, F.; Mueden, A. The creation of acid carbon surfaces by treatment with $(NH_4)_2S_2O_8$. Carbon. 1997, 35, 1619-1626. DOI: https://doi.org/10.1016/S0008-6223(97)00121-8

[35] Ishizaki, C.; Marti, I. Surface oxide structures on a commercial activated carbon. Carbon. 1981, 19, 409-412. DOI : https://doi.org/10.1016/0008-6223(81)90023-3

[36] Papirer, E.; Guyon, E.; Perol, N. Contribution to the study of the surface groups on carbons—II: Spectroscopic methods. Carbon. 1978, 16, 133-140. DOI: https: // doi.org/ 10.1016/0008-6223(78)90010-6

[37] Djilani, C.; Zaghdoudi, R.; Modarressi, A.; Rogalski, M. ; Djazi, F.; Lallam, A. Elimination of organic micropollutants by adsorption on activated carbon prepared from agricultural waste. Chem. Engin. J. 2012, 189-190, 203-212. DOI: https: // doi.org/ 10.1016/j.cej.2012.02.059

[38] Koutcheiko, S.; Monreal, C.M.; Kodama, H.; McCracken, T.; Kotlyar, L. Preparation and characterization of activated carbon derived from the thermo-chemical conversion of chicken manure. Bioresour. Technol. 2007, 98, 2459- 2464. DOI: https://doi.org/10.1016/j.biortech.2006.09.038

[39] Saldarriaga, J.F.; Aguado, R.; Pablos, A.; Amutio, M.; Olazar, M.; Bilbao, J. Fast characterization of biomass fuels by thermogravimetric analysis (TGA). Fuel, 2015, 140, 744–751. DOI : https://doi.org/10.1016/j.fuel.2014.10.024.

[40] Djilani, C.H.; Zaghdoudi, R.; Modarressi, A.; Rogalski, M.; Djazi, F.; Lallam, A. Elimination of organic micropollutants by adsorption on activated carbon prepared from agricultural waste. Chem. Eng. J. 2012 ; 189–190, 203–212. DOI : https://doi.org/10.1016/j.cej.2012.02.059

[41] Le Vann, K.; Thuy Luong Thi, T. Activated carbon derived from rice husk by NaOH activation and its application in supercapacitor. Prog. Nat. Sci. 2014, 24, 191-198. DOI : https://doi.org/10.1016/j.pnsc.2014.05.012

[42] Zubir, M.H.M. ; Zaini, M.A.A. Twigs-derived activated carbons via $H_3PO_4/ZnCl_2$ composite activation for methylene blue and congo red dyes removal. Sci Rep. 2020, 10, 14050. DOI : https://doi.org/10.1038/s41598-020-71034-6

[43] Ghorbani, F.; Kamari, S.; Zamani, S.; Akbari, S.; Salehi, M. Optimization and modeling of aqueous Cr(VI) adsorption onto activated carbon prepared from sugar beet bagasse agricultural waste by application of response surface methodology. Surf. Interfaces, 2020, 18, 100444. DOI : https://doi.org/10.1016/j.surfin.2020.100444

[44] Üner, O.; Geçgel, Ü.; Bayrak, Y. Adsorption of Methylene Blue by an Efficient Activated Carbon Prepared from Citrullus lanatus Rind: Kinetic, Isotherm, Thermodynamic, and Mechanism Analysis. Water Air Soil Pollut. 2016, 227, 247. DOI : https://doi.org/10.1007/s11270-016-2949-1

[45] Puri, B.R. in Walker, P.L.; Jr. editor. Chemistry and physics of carbon. New York, Marcel Dekker, 1966, p. 161.

[46] Mall, I.D.; Srivastava, V.C.; Agarwal, N.K. Removal of Orange-G and Methyl Violet dyes by adsorption onto bagasse fly ashdkinetic study and equilibrium isotherm analyses. Dyes Pigm. 69 (2006) 210-223. DOI : https://doi.org/10.1016/j.dyepig.2005.03.013

[47] Satyavani, T.V.S.L. ; Ramya Kiran, B. ; Rajesh Kumar, V. ; Srinivas Kumar, A.; Naidu, S.V. Effect of particle size on dc conductivity, activation energy and diffusion coefficient of lithium iron phosphate in Li-ion cells. Eng. Sci. Technol. 2016, 19, 40-44. DOI : https://doi.org/10.1016/j.jestch.2015.05.011

[48] McCarter, W.J.; Starrs, G.; Chrisp, T.M.; Banfill, P.F.G. Activation energy and conduction in carbon fibre reinforced cement matrices. J. Mater. Sci. 2007, 42, 2200–2203. DOI : https://doi.org/10.1007/s10853-007-1517-x

[49] Güler, O.; Yavuz, Ç.; Başgöz, Ç.; Altın, S.; Yahia, I.S. Efect of carbon nanotubes/graphene nanoplates hybrid to ZnO matrix: production, electrical and optical

properties of nanocomposite. J. Mater. Sci.: Mater. Electron. 2020, 31, 3184–3196. DOI : https://doi.org/10.1007/s10854-020-02866-1

[50] Trihotri, M.; Dwivedi, U.K.; Khan, F.H.; Malik, M.M.; Qureshi, M.S. Effect of curing on activation energy and dielectric properties of carbon black–epoxy composites at different temperatures. J. Non-Cryst. Solids 2015, 421, 1-13. DOI : https://doi.org/10.1016/j.jnoncrysol.2015.04.020

[51] Tchernij, S.D.; Skukan, N.; Picollo, F.; Battiato, A.; Grilj, V.; Amato, G.; Boarino, L.; Enrico, E.; Jakšić, M.; Olivero, P.; Forneris, J. Electrical characterization of a graphite-diamond-graphite junction fabricated by MeV carbon implantation. Diam. Relat. Mater. 2017, 74, 125-131.DOI : https://doi.org/10.1016/j.diamond.2017.02.019

[52] Bard, A.J.; Faulkner, L.R. Electrochemical Methods-Fundamentals and Applications, 2nd edition, New York (USA), John Wiley and Sons Inc., 2001.

[53] Kang, W.; Pei, X.; Rusinek, C.A.; Bange, A.; Haynes, E.N.; Heineman, W.R.; Papautsky, I. Determination of Lead with a Copper-Based Electrochemical Sensor. Anal. Chem. 2017, 89, 3345–3352. DOI : https://doi.org/10.1021/acs.analchem.6b03894

[54] International Union of Pure and Applied Chemistry (IUPAC). Nomenclature, symbols, units and their usage in spectrochemical analysis—II. data interpretation Analytical chemistry division, Spectrochim. Acta, Part B, 1978, 33, 241-245. DOI : https://doi.org/10.1016/0584-8547(78)80044-5.

[55] Benedito da Silva, O.; Machado, S.A.S. Evaluation of the detection and quantification limits in electroanalysis using two popular methods: application in the case study of paraquat determination, Anal. Methods. 2012, 4, 2348. DOI : https://doi.org/10.1039/C2AY25111F

[56] Ziyatdinova, G.K.; Ziganshina, E.R.; Nguyen, C.; Budnikov, H.C. Determination of the Antioxidant Capacity of the Micellar Extracts of Spices in Brij® 35 Medium by Differential

Pulse Voltammetry. J. Anal. Chem. 2016, 71, 573–580. DOI: https // doi.org/ 10.1134/S1061934816060174.

[57] Badea, M.; Di Modugno, F.; Floroian, L.; Mirela Tit, D.; Restani, P.; Bungau, S.; Iovan, C.; Badea, G.E.; Aleya, L. Electrochemical strategies for gallic acid detection: Potential for application in clinical, food or environmental analyses. Sci. Total Environ. 2019, 672, 129-140. DOI: 10.1016/j.scitotenv.2019.03.404

List of tables

Table 1. Infrared spectral data of carbon compounds.

Table 2. Detection limits of gallic acid and the sensitivity of the different modified electrodes.

Figure captions

Fig. 1. SEM images of : (a) horizontal cross section of AC ; (b) vertical cross section of AC ; (c) and (d) CSs/AC-CNTs.

Fig. 2. Diffractograms of the different carbon compounds.

Fig. 3. Thermograms (TGA) of the different carbon compounds.

Fig. 4. Conductivity behavior of the different carbon compounds : (a) S=f(T) ; (b) and (c) log(S) =f(1000/T).

Fig. 5. Cyclic voltamperograms of carbon compounds recorded using modified carbon paste electrode in NaH_2PO_4/Na_2HPO_4 (0.1 M); KNO_3 (0.1M) : (a) in the absence of GA ; (b) in the presence of GA (0.01M).

Fig. 6. Electrochemical study at different scan rate in NaH_2PO_4/Na_2HPO_4 (0.1M) ; KNO_3 (0.1M) ; concentration of GA 0.01M : (a) Cyclic voltamperogram obtained using GC/CSs/AC-CNTs; (b) Current vs. square root of scan rate; (c) logv vs. potential.

Fig. 7. Square wave voltamperograms recorded using cavity microelectrode (CME) modified with GC/CA, GC/AC-CNTs and GC/CSs/AC-CNTs compounds in NaH_2PO_4/Na_2HPO_4 (0.1 M); KNO_3 (0.1M) in the presence of GA (0.0053M).

Fig. 8. (a) Square wave voltamperograms recorded using GC/CSs/AC-CNTs electrode and calibration plots at different concentration of gallic acid using: (b) GC/CSs/AC-CNTs ; (c) GC/AC and GC/AC-CNTs electrodes in NaH_2PO_4/Na_2HPO_4 (0.1 M) and KNO_3 (0.1M).

Fig. 9. (a) Square wave voltamperograms recorded using CME/GC/CSs/AC-CNTs electrode and calibration plots at different concentration of gallic acid in NaH_2PO_4/Na_2HPO_4 (0.1 M) and KNO_3 (0.1M).

Fig. 10. (a) Square wave voltamperograms recorded using four CME/GC/CSs/AC-CNTs electrodes in NaH_2PO_4/Na_2HPO_4 (0.1 M) and KNO_3 (0.1M) in the presence of GA (0.00192M).

Fig. S1. FT-IR Spectra of AC, AC-CNTs and CSs/AC-CNTs.

Fig. S2. EDX analysis of: (a) AC-CNTs; (b) CSs/ AC-CNTs

Fig. S3. Electrochemical study at different scan rate in NaH_2PO_4/Na_2HPO_4 (0.1M) ; KNO_3 (0.1M) ; concentration of GA 0.01M . (a) Current vs. square root of scan rate and (b) Potential vs. Log v recorded with GC/AC-CNTs electrode.

Fig. S4. Potential vs. Log v recorded with GC/AC electrode in NaH_2PO_4/Na_2HPO_4 (0.1M) ; KNO_3 (0.1M) ; concentration of GA 0.01M.

Fig. S5. Square wave voltamperograms recorded using carbon paste electrodes modified by the carbon materials in NaH_2PO_4/Na_2HPO_4 (0.1 M); KNO_3 (0.1M) in the absence (0 M) and the presence of GA (0.01 M).

Table 1. Infrared spectral data of carbon compounds.

FT-IR (ATR) attribution	Coal	AC	CNTs	CSs	AC-CNTs	CSs/AC-CNTs
$\bar{\nu}_{\text{OH hydroxyl and carboxyl}}$	3425	3403	3410	3401	3424	3424
$\bar{\nu}_{\text{CH2 or CH3 asym}}$	2928	2921	2922	2922	2928	2923
$\bar{\nu}_{\text{CH2 and CH3 sym}}$	2859	2849	2852	2854	2855	2854
$\bar{\nu}_{\text{C=C aromatic ring}}$	1577	1564	1555	1579	1563	1545
$\bar{\nu}_{\text{C=O carboxylic acid}}$	1733	1739	1739	1721	1752	1724
$\delta_{\text{O-H hydroxyl and carboxyl}}$	1384	1378	1382	1395	1384	1382
$\delta_{\text{CH in CH3}}$	1430	1424	1460	1433	1441	1442
$\bar{\nu}_{\text{C-O hydroxyl and carboxyl}}$	1118	1134	1113	1148	1221	1221

ν: Stretching vibration; δ: Deformation vibration; FTIR: Fourier transform infrared spectroscopy; ATR: Attenuated total reflectance; AC: Activated carbon; CNTs : Carbon nanotubes ; CSs : Carbon sphers.

Table 2. Detection limits of gallic acid and the sensitivity of the different modified electrodes.

Electrodes	pH	Linear range ($\times 10^{-3}$ M)	LOD (μM)	References
GCE/CeO_2 nanoparticles	7.4	0.050-2.49	11.9	[56]
Screen-printed carbon electrodes	7.0	0.1-2.00	23-102	[57]
Redox microsensors	7.0	0.1-2.0	109	[57]
GC/AC	7.0	0-5.36	22.86	This work
GC/AC-CNTs	7.0	0-5.36	8.11	This work
GC/CSs/AC-CNTs	7.0	0-5.36	6.43	This work
CME/GC/CSs/AC-CNTs	7.0	0-5.36	3.64	This work

LOD : Limit of detection ; GCE : Glassy carbon electrode ; AC: Activated carbon; CNTs : Carbon nanotubes ; CSs : Carbon sphers ; CME : Cavity microelectrode.

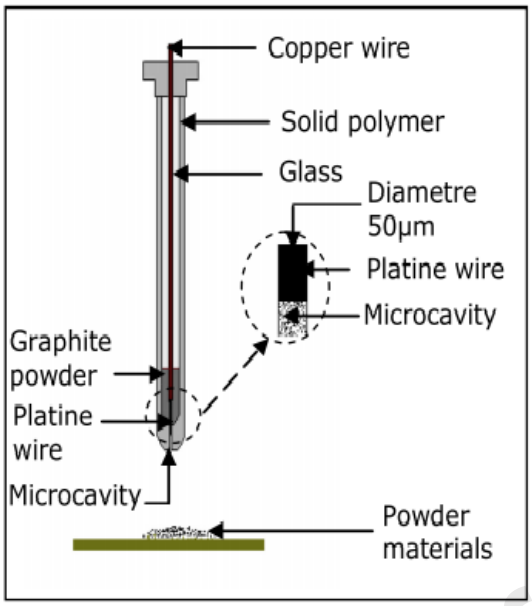

Scheme 1. Representation of the cavity microelectrode (CME)

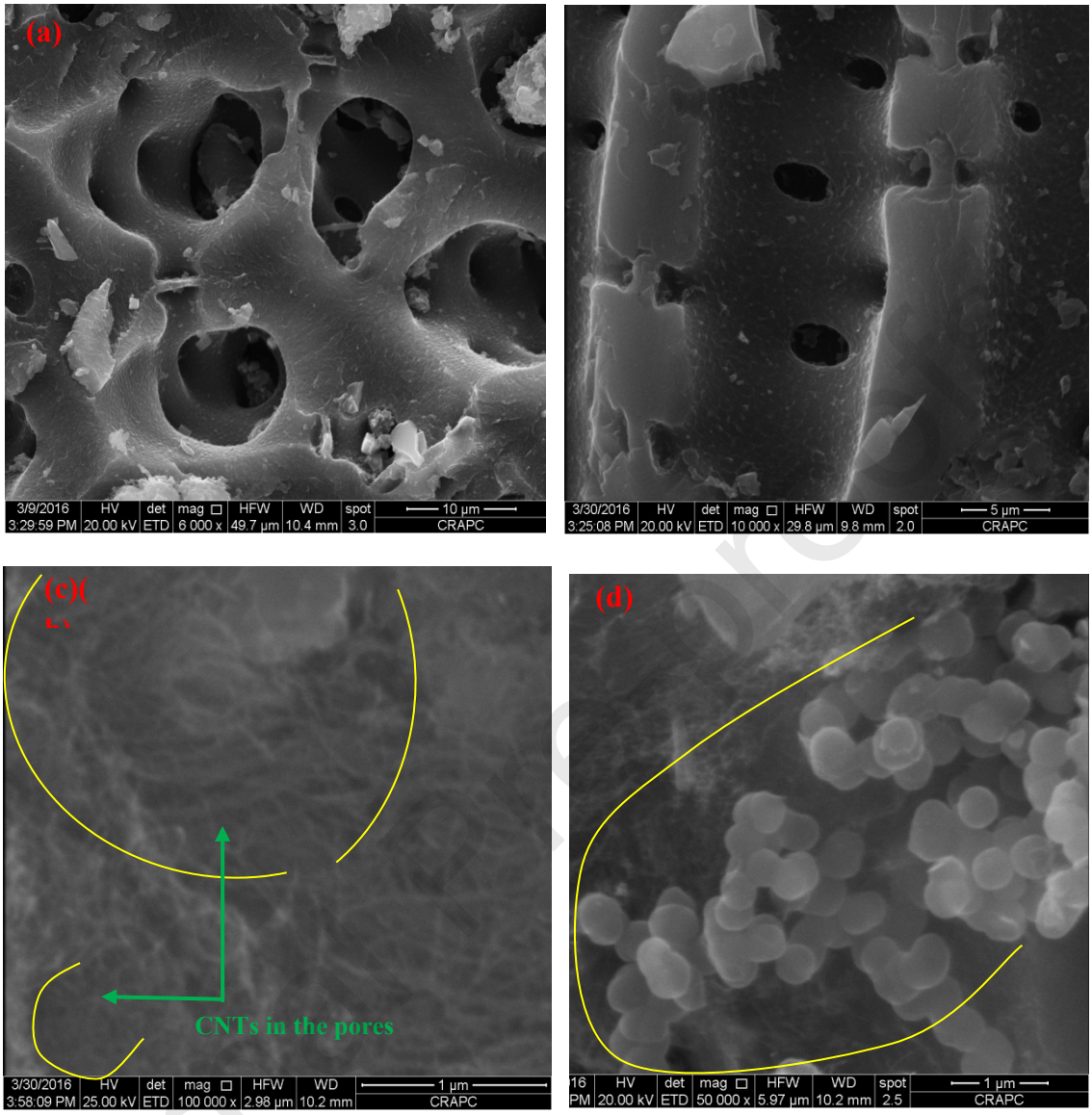
(a)
3/9/2016 3:29:59 PM | HV 20.00 kV | det ETD | mag 6 000 x | HFW 49.7 µm | WD 10.4 mm | spot 3.0 | 10 µm | CRAPC
3/30/2016 3:25:08 PM | HV 20.00 kV | det ETD | mag 10 000 x | HFW 29.8 µm | WD 9.8 mm | spot 2.0 | 5 µm | CRAPC
(c)(
CNTs in the pores
3/30/2016 3:58:09 PM | HV 25.00 kV | det ETD | mag 100 000 x | HFW 2.98 µm | WD 10.2 mm | 1 µm | CRAPC
(d)
16 PM | HV 20.00 kV | det ETD | mag 50 000 x | HFW 5.97 µm | WD 10.2 mm | spot 2.5 | 1 µm | CRAPC

Fig. 1.

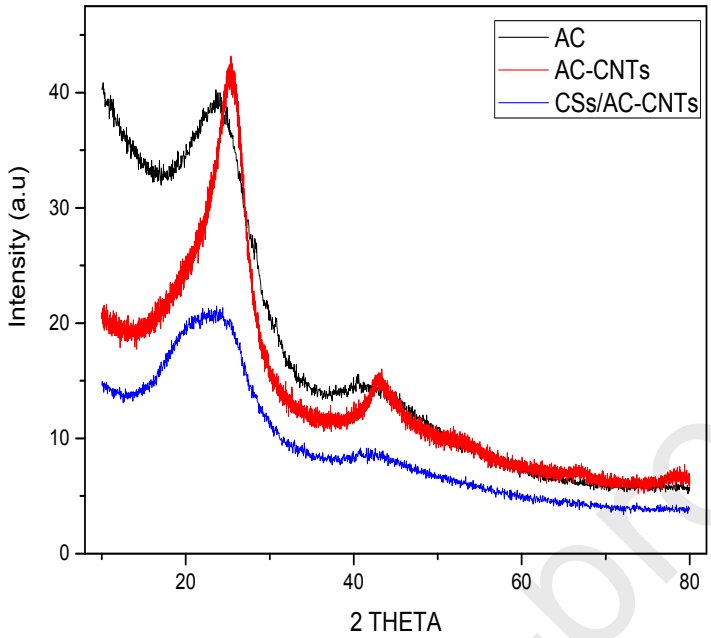

Fig. 2.

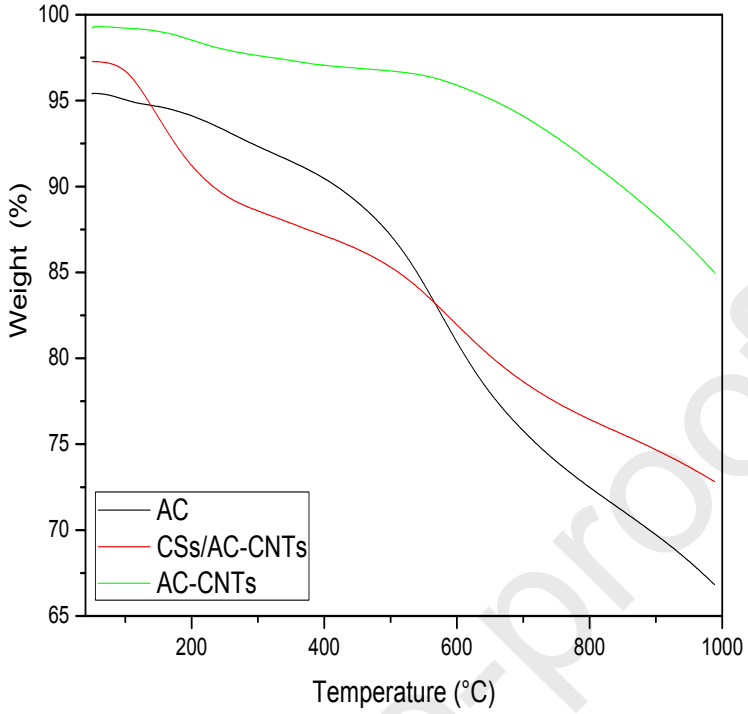

Fig. 3.

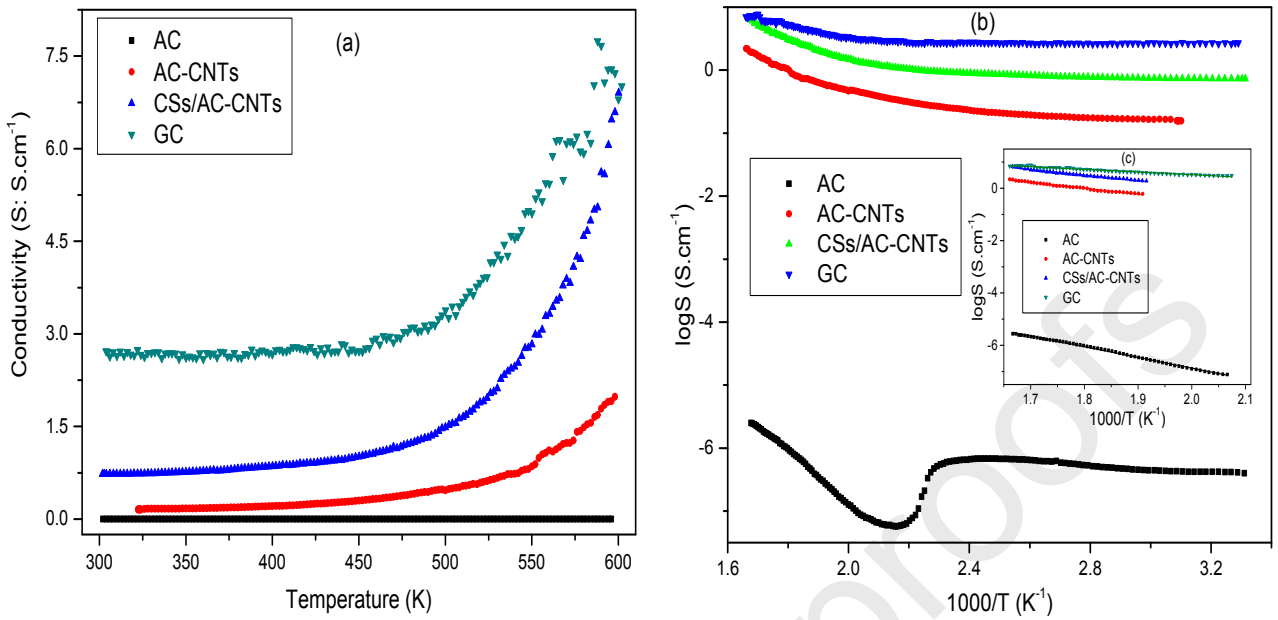

Fig. 4.

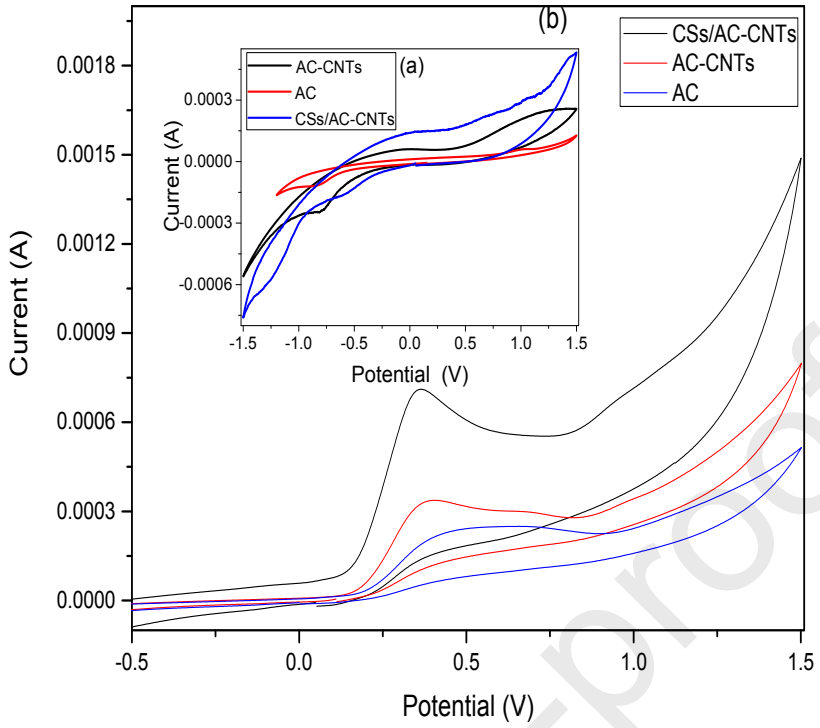

Fig. 5.

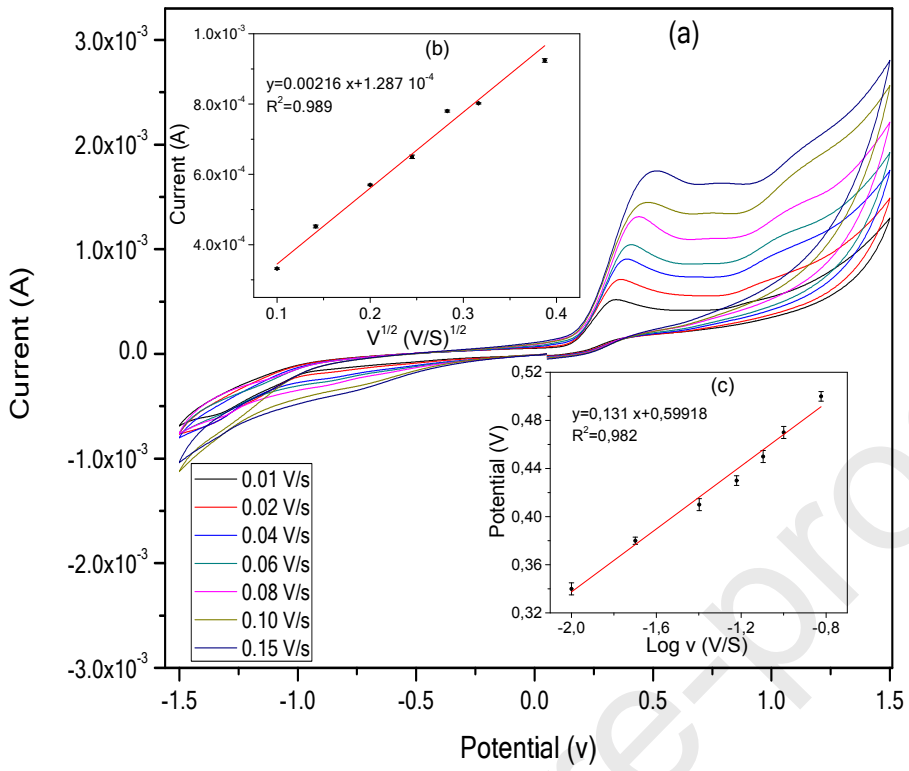

Fig. 6.

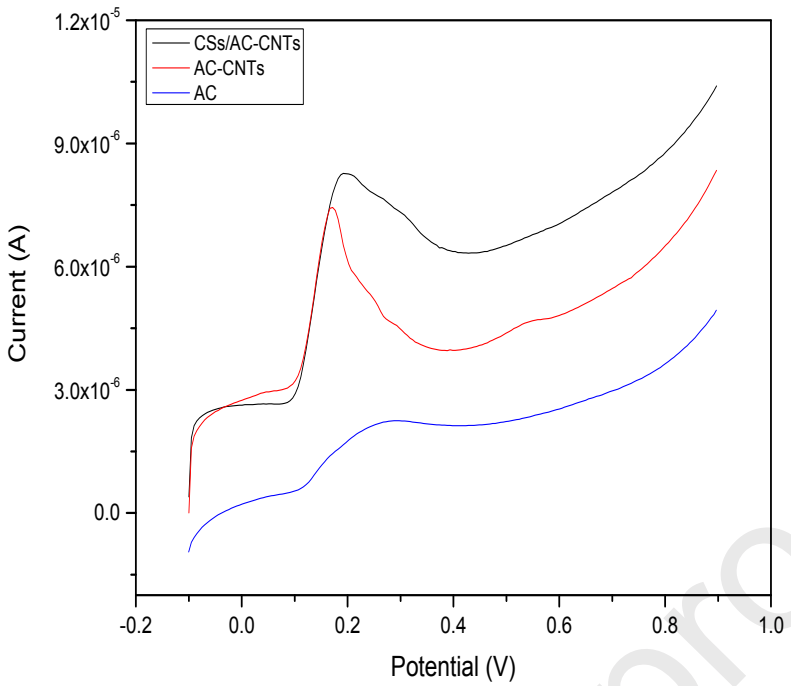

Fig. 7.

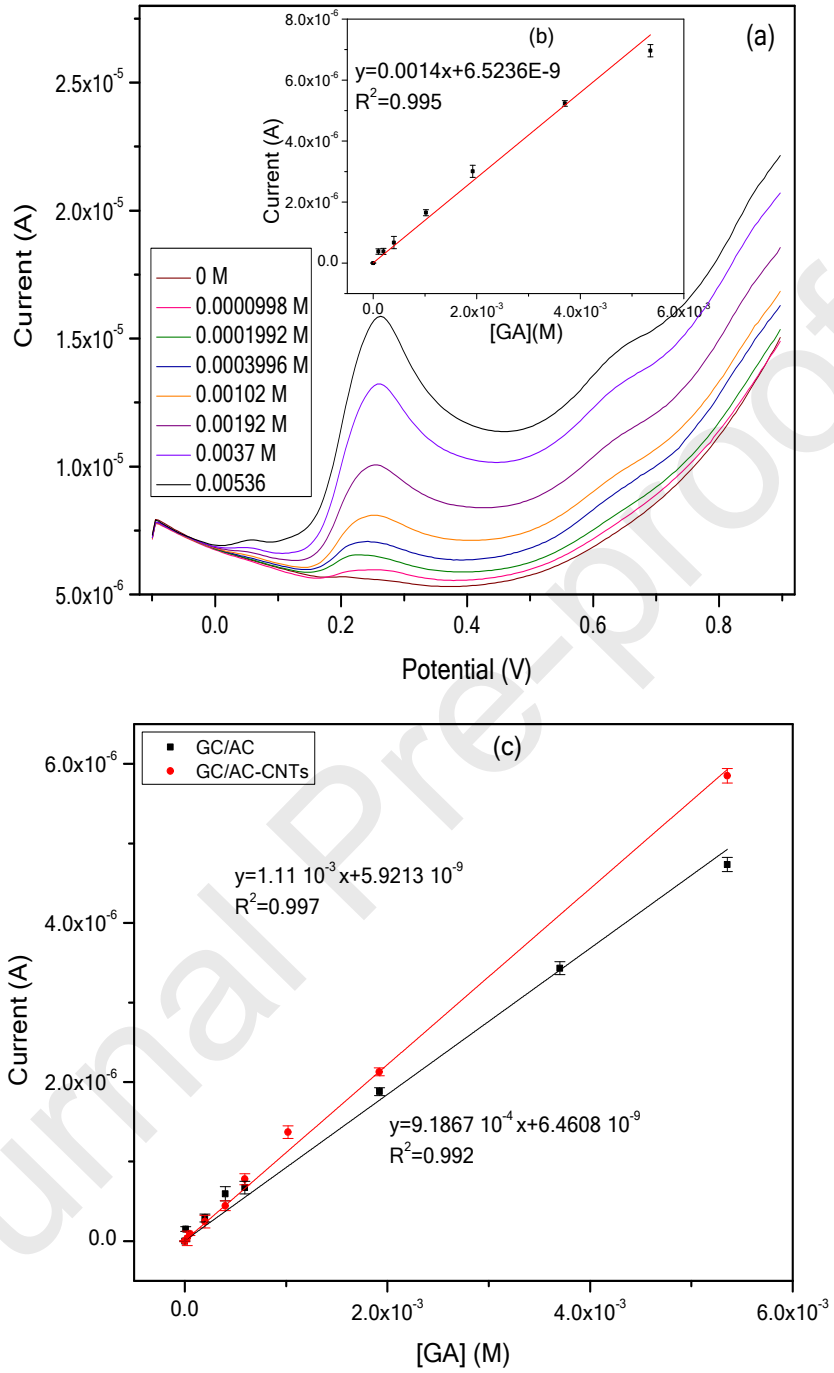

Fig. 8.

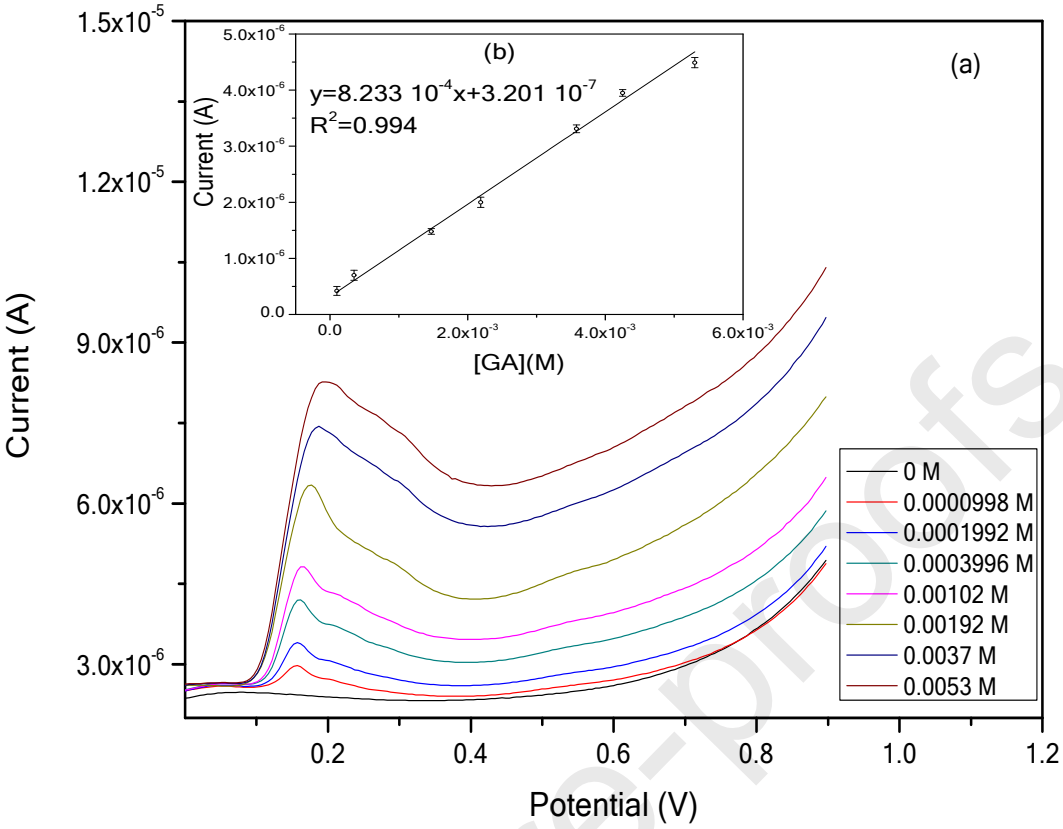

Fig. 9.

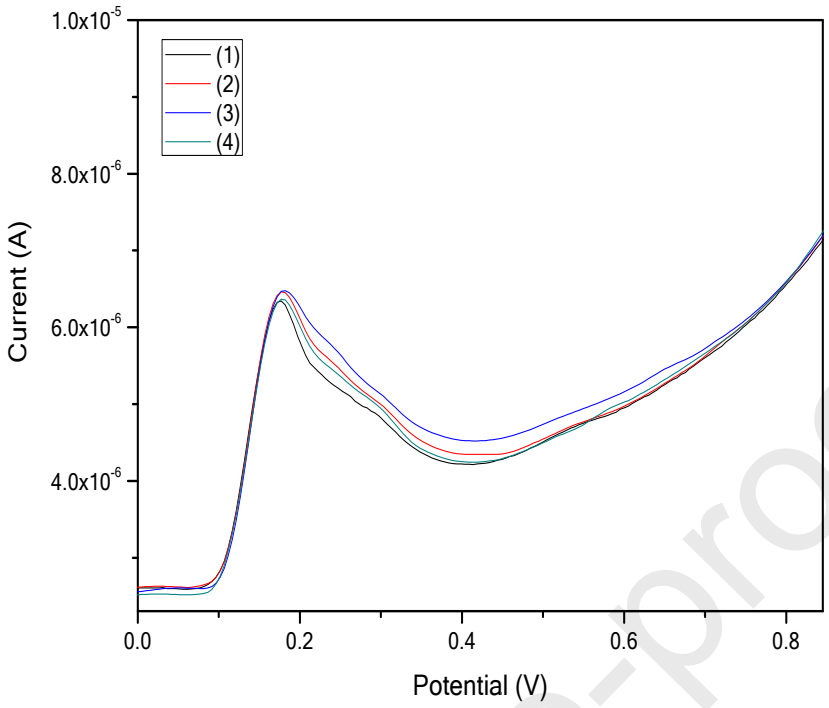

Fig. 10.

Graphical abstract

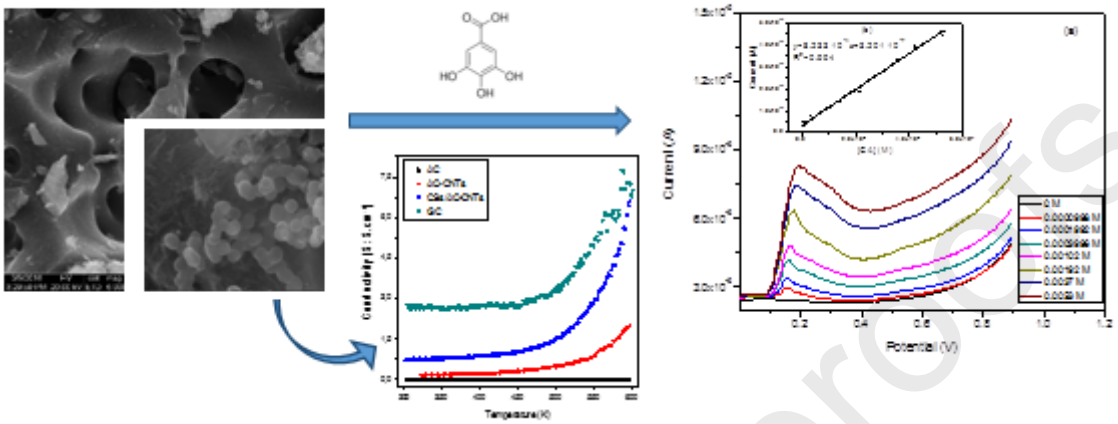

Highlights

- Electrical conductivity measurements were reported for new hybrid carbon materials based on activated carbon (AC), carbon spheres (CSs) and carbon nanotubes (CNTs).
- CSs/AC-CNTs hybrid carbon material shows highest electrical conductivity and lowest activation energy.
- The charge transfer coefficient reveals a better electro-catalytic oxidation mechanism of gallic acid.
- The cavity microelectrode (CME) modified with CSs/AC-CNTs exhibits a lower limit of detection of gallic acid.
- The reproducibility and stability of CME/CSs/AC-CNTs revealed that the RSD % of gallic acid response was about 1.44 and 3.7 %, respectively.

Credit author statement

Achour TERBOUCHE: Conceptualization, Methodology, Writing-Original draft preparation, Supervision, Validation, Reviewing and Editing.

Soumeya BOULAHIA and Sarah MECERLI: Working, Analysis.

Chafia AIT-RAMDANE-TERBOUCHE: Substantial contribution to research design, The acquisition, Interpretation of Infrared and thermal analysis data.

Hakim BELKHALFA: Analysis, Interpretation of SEM-EDX and XRD analysis data.

Djamila GUERNICHE: Substantial contribution to carbon materials synthesis, Interpretation of electrical conductivity measurements.

Moussa SEHAILIA: Writing, Reviewing.

Khaldoun BACHARI: The acquisition, Reviewing, Visualization.

Djillali MEZAOUI: Conceptualization, Methodology, Supervision and Validation.

Didier HAUCHARD: Methodology, Interpretation of the electrochemical results.

Declaration of interests

☒ The authors declare that they have no known competing financial interests or personal relationships that could have appeared to influence the work reported in this paper.

☐The authors declare the following financial interests/personal relationships which may be considered as potential competing interests: